

# Modulated Photoconductivity in YB<sub>66</sub>

Yoshiko Sakairi, Masatoshi Takeda, and Kaoru Kimura

*Department of Materials Science, The University of Tokyo, 7-3-1 Hongo, Bunkyo-ku, Tokyo 113, Japan*

and

Takaho Tanaka

*National Institute for Research in Inorganic Materials, 1-1 Namiki, Tsukuba, Ibaragi 305, Japan*

Received April 7, 1997; accepted April 10, 1997

---

**The modulated photoconductivity was measured in single crystal YB<sub>66</sub>, essentially consisting of B<sub>12</sub> icosahedral clusters like many other boron-rich borides. A model, in which localized states participate both in photocarrier generation and trapping well explains the phase shift between excitation and photocurrent. For the localized states involved, an ionization energy of 0.19 eV is estimated.** © 1997 Academic Press

---

## INTRODUCTION

The physical properties and the electronic structures of boron and boron-rich borides have characteristics reminding of disordered solids, which characteristics are assigned to B<sub>12</sub> clusters constructing their structures (1). Among these materials YB<sub>66</sub> has the largest unit cell with more than 1600 atoms (2), suggesting a higher disorder of B<sub>12</sub> clusters than in simpler boron and boride structures. Up to now, only few physical properties of single crystal YB<sub>66</sub> have been reported (3, 4), e.g., the electrical conductivity describable by Mott's law of variable-range hopping and the edge absorption reminding of the Urbach tail of amorphous semiconductors. The electronic structure has remained unsolved.

In the present study, localized states and carrier generation in YB<sub>66</sub> were analyzed by modulated photocurrent (MPC) measurements determined by carrier generation, trapping in localized states, reexcitation, and recombination (5, 6).

## EXPERIMENT

A high-quality single crystal was prepared by an indirect heating floating zone method; the chemical composition of the feed rod was [B]/[Y] = 56. For sample preparation,

see Ref. (7). The ingot was sliced and the surfaces were high grade polished (about 1 cm in diameter and 1 mm in thickness).

For excitation the chopped light of an Ar-ion laser (488.8 nm, 2.54 eV) illuminated the surface area between two evaporated aluminum electrodes. By lock-in technique amplitude and phase of the modulated photocurrent were simultaneously measured. The frequency dependence of the amplitude and the phase induced by the apparatus were corrected according to reference measurements with a fast Si-photodiode (see Fig. 1). The modulation frequency was varied from 5 to 3500 Hz.

## RESULTS AND DISCUSSION

Frequency dependence of amplitude and phase shift of the photocurrent at several temperatures are shown in Figs. 2a and 2b. A first attempt to describe the results by a simple model (5), taking interband excitation, trapping in localized states, reexcitation, and recombination via recombination states into account, was not successful. Therefore the results were analyzed with a model (6) considering two kinds of carrier generation: (i) photoexcitation directly into the conduction band and (ii) photoexcitation to localized states near the conduction band and subsequent thermal excitation into the conduction band (see Fig. 3). Although it is assumed in Fig. 3 that photocarriers are electrons in the conduction band, the model also holds if the photocarriers are holes in the valence band. Then the phase shift consists of two parts,

$$\phi_1 = \tan^{-1} \omega \tau z, \quad [1]$$

$$\phi_2 = \tan^{-1} \frac{(K_2/K_1)(\omega/P_s)}{1 + (K_2/K_1) + (\omega/P_s)^2}, \quad [2]$$

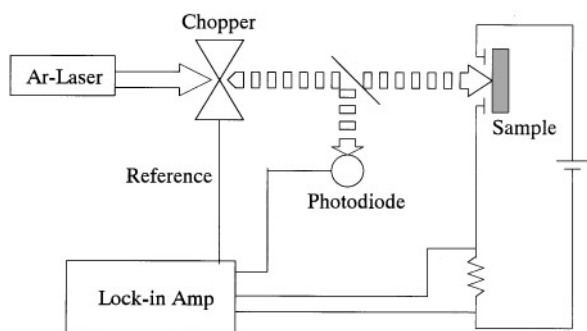


FIG. 1. Block diagram of the setup for measuring the modulated photoconductivity.

where  $K_1$  and  $K_2$  are the excitation rates of the processes indicated in Fig. 3,  $P_s \propto \exp(E_s/kT)$  is thermal excitation rate from the localized states into the conduction band (ionization energy,  $E_s$ ),  $\omega$  is the modulation angular frequency,  $\tau$  is frequency dependent effective recombination time, and  $z$  is related to trapping and reexcitation of carriers. Equations [1] and [2] show that  $\phi_1$  is associated only with the transport processes and  $\phi_2$  only with the carrier generation processes.

The frequency dependence of  $\phi_2$  exhibits a maximum moving toward lower frequencies, when the temperature decreases because  $P_s$  is proportional to  $\exp(E_s/kT)$ . A plot of  $\phi_2$  as a function of  $\omega/P_s$  yields the temperature independence of  $\phi_2$ . Then the results in Fig. 2b can be normalized as shown in Fig. 4 by moving the phase shift curves along the

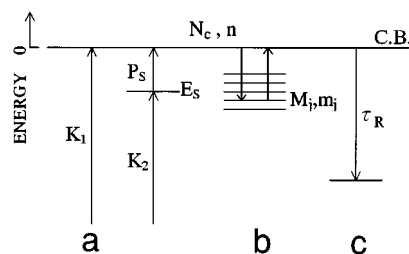


FIG. 3. Energy level scheme for the model of the modulated photoconductivity, showing the energy level locations and the process taken into account.

horizontal axis using a temperature-dependent normalizing factor,  $1/P_s$ . Temperature dependence of this factor assigned an activation energy of 0.19 eV (Fig. 5). This is the ionization energy of the localized state.

According to these results two energy band schemes for YB<sub>66</sub> seem possible:

(i) a mobility gap of 2.73 eV equal to the sum of the optical excitation energy (2.54 eV) and the thermal activation energy (0.19 eV) that is very large when compared with the absorption spectrum exhibiting at 0.7 eV an absorption coefficient of  $10^3 \text{ cm}^{-1}$  (3);

(ii) a large density of localized states in a distance of 0.19 eV from the mobility edge, so that the carrier excitation into these localized states makes a large contribution toward the photoconduction process even if the photon energy is larger than the mobility gap.

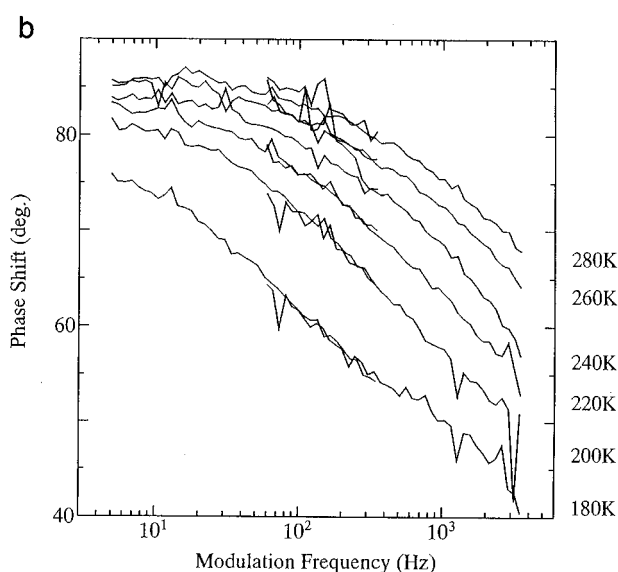
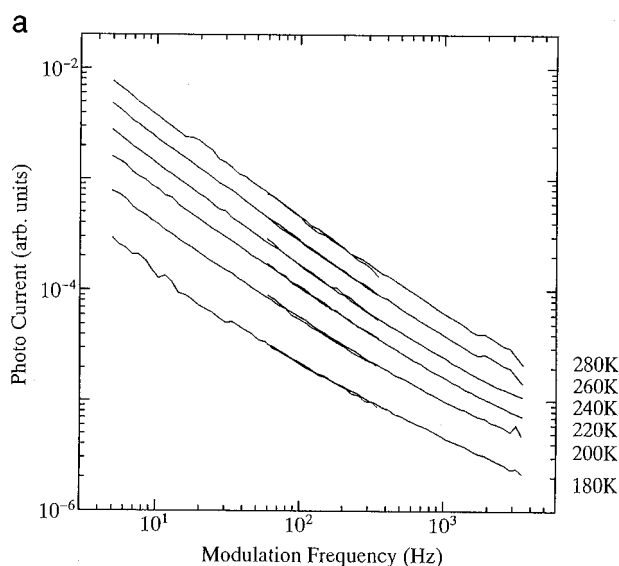


FIG. 2. Modulation frequency dependence of photocurrent (a) and phase shift (b) of single crystal YB<sub>66</sub> measured at several temperatures.

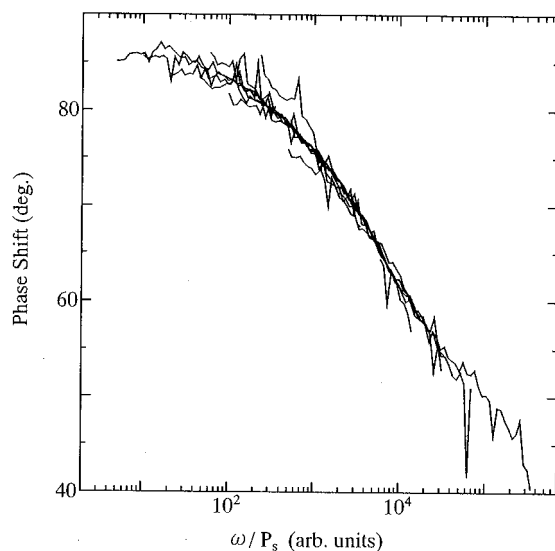


FIG. 4. The particular curve of the phase shift, appearing when the results of the modulation frequency dependence at respective temperatures are moved along the horizontal axis to coincide with the result at 280 K. This procedure corresponds to the conversion of horizontal axis from  $\omega$  into  $\omega/P_s$ .

The present results do not allow differentiation between the two band schemes. However, it is sure that the localized states within the band gap play an important role in the photoconduction process.

#### ACKNOWLEDGMENTS

One of the authors (M. Takeda) acknowledges Research Fellowships of the Japan Society for the Promotion of Science for Young Scientists. This work has been supported by a Grant-in-Aid from the Ministry of Education, Science, and Culture.

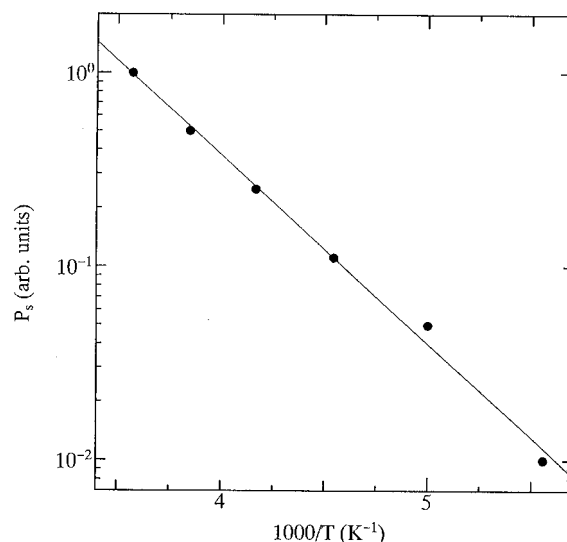


FIG. 5. Temperature dependence of the factor corresponding to the thermal release rate  $P_s$  (see text).

#### REFERENCES

1. e.g., R. Frantz and H. Werheit, in "Boron-rich Solids" (D. Emin, T. Aserage, A. C. Switendick, B. Morosin, and C. L. Beckel, Eds.), AIP Conf. Proc. 231, p. 29. AIP, New York, 1991.
2. S. M. Richards and J. S. Kasper, *Acta Crystallogr.* **25**, 237 (1969).
3. U. Kuhlmann, H. Werheit, J. Hassdenteufel, and T. Tanaka, *Jpn. J. Appl. Phys. Series* **10**, 82 (1994).
4. O. A. Golikova, in "Boron-rich Solids" (D. Emin, T. Aserage, A. C. Switendick, B. Morosin, and C. L. Beckel, Eds.), AIP Conf. Proc. 231, p. 108. AIP, New York, 1991.
5. H. Oheda, *J. Appl. Phys.* **52**, 6693 (1981).
6. H. Oheda, *Solid State Commun.* **33**, 203 (1980).
7. T. Tanaka, Y. Ishizawa, J. Wong, Z. U. Rek, M. Rowen, F. Schäfers, and B. R. Müller, *Jpn. J. Appl. Phys. Series* **10**, 110 (1994).